

A NEW APPROACH TO SPATIO-TEMPORAL CALIBRATION OF MULTI-SENSOR SYSTEMS

M. Blázquez

Institute of Geomatics
Generalitat de Catalunya & Universitat Politècnica de Catalunya
Parc Mediterrani de la Tecnologia
Av. del Canal Olímpic s/n, Castelldefels, Spain
marta.blazquez@ideg.es

KEY WORDS: photogrammetry, calibration, spatio-temporal, modeling, orientation, sensor, INS/GPS

ABSTRACT:

The purpose of this paper is to propose new, rigorous, more robust and reliable models and methods for the calibration and orientation of multi-sensor systems with INS/GPS data. On the one hand, the classical spatial sensor orientation and calibration problem is reformulated as a relative control problem by transferring the relative orientation of an Inertial Measurement Unit (IMU) between two epochs to the relative orientation of a rigidly attached sensor between the same two epochs. This approach eliminates the need for the IMU-to-sensor relative orientation [boresight] calibration parameter. On the other hand, a rigorous 4D —spatio-temporal— model, based on the full exploitation of the INS/GPS-derived control data, is introduced. The paper discusses the key ideas behind both proposed approaches, presents the corresponding mathematical models, identifies some of their advantages, and demonstrates their potential through real data.

1 INTRODUCTION

Nowadays, the use of INS/GPS time, position and attitude (tPA) derived information as aerial control to support sensor orientation and calibration is a well-established procedure (Lucas, 1987, Schwarz et al., 1993). For some sensor designs, the use of tPA aerial control is a must. For others, it is just an option; be it for the purpose of better geometric accuracy, for more flexible mission design or just to match competitors' equipment. Whatever the reason is, INS/GPS instrumentation has become a "de facto" standard companion to the mapping sensors. This situation, in turn, has consolidated two well-defined calibration and orientation procedures: Direct Sensor Orientation (DSO) and the so-called Integrated Sensor Orientation (ISO). In DSO, sensor position and attitude literally depend on INS/GPS-derived tPA control information. ISO does not depend from it, it just benefits from it.

DSO is the procedure that directly provides the orientation parameters of the sensor (Schwarz et al., 1993). ISO is the procedure that combines measurements on the mapping sensors' data with whatever other available control data in order to compute the sensor orientation parameters in a block adjustment (Ackermann and Schade, 1993, Frieß, 1991). In practice, most times, the ISO procedure is nothing else than a traditional aerial triangulation adjustment with tPA aerial control and a few ground control points. With this combination, the ISO procedure inherits the advantages of traditional block adjustment, reduces ground control and relaxes mission geometric constraints.

ISO is both an orientation and calibration procedure; i.e., the calibration and orientation parameters are estimated simultaneously in the block adjustment. On the other side — although this depends on the project and on the precision and accuracy requirements— DSO requires a previous ISO

step to calibrate the sensors and the sensor-system (Colomina, 1999).

The paper proposes new 3D models for the traditional ISO procedure. The proposed models, more robust and reliable, are based on the fact that the relative attitude of the sensor between two epochs coincides with the relative orientation of the IMU between the same two epochs (assuming that the sensor and IMU are rigidly attached). This rationale brings us to the equations which model the orientation of the sensor in terms of the tPA aerial control without the need of the boresight calibration matrix (Blázquez and Colomina, 2008). Actual data are used to show the first results and demonstrate the potential of this approach.

The classical ISO models, algorithms, methods and procedures just tackle the spatial calibration aspects. However, experience tells that incorrect or just inaccurate time synchronization between sensors is a big troublemaker. While spatial calibration is dealt both at the HW and SW levels, temporal calibration —time synchronization— is left to the HW. This results in reasonable robust and resilient systems as for geometry and weak systems as for time. In other words, current models for sensor and sensor-system calibration are 3D —restricted to geometry— while the problem is a genuine 4D, spatio-temporal one (Blázquez and Colomina, 2008).

The paper also proposes models and methods to solve the above 4D problem. In this sense, the contribution of the paper is twofold: firstly, genuine spatio-temporal orientation and calibration models are derived and, secondly, appropriate observational control data (for example, INS/GPS velocity) are identified for the precise estimation of the 4D model parameters.

In a multi-sensor system there are two types of time errors: individual sensor internal errors and system synchro-

nization ones. In the case of individual sensor errors, the calibration method must be based on particular mathematical models of the sensor. In the other case, even if all the sensor oscillators are “perfect,” inaccurate time synchronization between the various system sensors can spoil the system performance and the sensor-system inconsistencies must be modeled. It is often the case, that individual sensor time drifts are dominated by external GPS receiver-generated precise [ambiguous] time pulses and that, for various technical and commercial reasons, inter-sensor constant temporal shifts occur. The paper focuses on the modeling of the sensor-system time synchronization problem.

For the estimation of the temporal calibration parameters, the use of the full INS/GPS-derived control data is proposed. In fact, INS/GPS delivers not only time, position and attitude (tPA) but also velocity (tPVA). These velocities can be used for calibrating the time errors and for decorrelating them from the space errors. This general principle is valid for any multi-sensor system and, in the paper, is formulated for the frame camera sensors.

The paper concludes by reporting on preliminary results of actual data tests performed for concept validation purposes. The results indicate that the new models make sense, behave as expected and deliver good results.

2 AERIAL CONTROL MODELS

2.1 Classical Aerial Control Models Extensions

The classical ISO procedure optimally estimates multi-sensor system parameters (unknowns) in the sense of least-squares relating observations (measurements) with these parameters through models. These models can be sensor models or aerial control models. The first ones are composed by the equations that model the own sensor behavior (sensor observations and its own orientation and calibration parameters). One example of sensor model is the collinearity equations. The second ones are composed by the equations which model the relation between the sensor, the GPS antenna receiver, and the IMU. The improvement of the classical aerial control mathematical functional models is the focus of this research.

The classical aerial control model relates tPA aerial control with the sensor orientation parameters, sensor-to-GPS antenna receiver parameters and sensor-to-IMU parameters for each epoch. In this paper, this model is referred to as spatial absolute aerial control model. Based on the following two obvious facts the classical aerial control models can be extended:

1. *The sensor calibration and orientation problem is not a 3D spatial problem, it is a 4D spatio-temporal one. Moreover, the INS/GPS-derived data contain not only positions and attitudes, they also contain velocities.*

2. *If a sensor and an IMU are rigidly attached, the sensor relative attitude between any two epochs is the same as the IMU relative attitude between the same two epochs.*

The extended model which takes into account the temporal dimension of the sensor orientation and calibration problem is referred to as spatio-temporal absolute aerial control model. This proposed model relates tPVA aerial control with the sensor orientation parameters, sensor-to-GPS antenna receiver parameters, sensor-to-IMU parameters, and multi-sensor time synchronization parameter for each epoch.

The extended model which takes into account the orientation and calibration problem for two epochs is referred to as spatial relative aerial control model. This proposed model relates tPA aerial control with the sensor orientation parameters, sensor-to-GPS antenna receiver parameters and sensor-to-IMU parameters for two epochs.

For the sake of completeness, the extended model which takes into account the temporal dimension of sensor orientation and calibration problem for two epochs is referred to as spatio-temporal relative aerial control model. This proposed model relates tPVA aerial control with the sensor orientation parameters, sensor-to-GPS antenna receiver parameters, sensor-to-IMU parameters, and multi-sensor time synchronization parameter for two epochs.

2.2 Naming and notation conventions

In the presented mathematical functional models, the involved reference frames and coordinate systems are listed in table 1.

l	Cartesian local terrestrial frame (east-north-up)
b	IMU instrumental frame (forward-left-up)
c	camera instrumental frame
l'	Cartesian local terrestrial frame (north-east-down)
b'	IMU instrumental frame (forward-right-down)
i	inertial reference frame

Table 1: Reference frames and coordinate systems.

If a variable x involves just one reference frame a , it is written x^a . If a variable involves two reference frames, the subscript symbol defines the “from” or “origin” (f) reference frame and the superscript symbol defines the “to” or “destination” (t) one like in x_f^t .

The observations and their residuals are denoted by lowercase symbols, a ; the parameters are denoted by uppercase symbols, A ; and the constant values (instrumental constant, observational auxiliary values, and constant rotation matrices) are denoted by the italic typestyle, a . The vector accent above a variable, \vec{a} , indicates that this variable is a 3-dimensional vector. For the sake of simplicity, $\vec{X}^f = (x, y, z)^f$ is used instead of the rigorous mathematical formulation $\vec{X}^f = [(x, y, z)^f]^T$. The observational residuals are denoted by the symbol v with the observation symbol as a subscript, for example, v_a denotes the residual of the observation a .

The eccentricity vector $\vec{A}^c = (a_x, a_y, a_z)^c$ from the camera projection centre to the GPS receiver antenna parameter; the $\vec{N}^c = (0, 0, n)^c$ constant vector, where n is the camera nodal distance; and the R_v^l rotation constant matrix are involved in all the mathematical functional models.

2.3 Absolute Aerial Control Models

Absolute aerial control functional models (spatial absolute aerial control models (2.3.1) and spatio-temporal absolute aerial control models (2.3.2)) involve the following observations and their residuals: the GPS- or INS/GPS-derived position, $\vec{x}^1 = (x, y, z)^1$ and the traditional [heading, pitch, roll] Euler angles, $\chi = (\psi, \vartheta, \gamma)$, that parameterize the $R_{b'}^1$ rotation matrix. In both absolute aerial control models, the involved parameters are: the camera projection centre, $\vec{X}^1 = (X, Y, Z)^1$; the traditional Euler angles, $\Gamma = (\omega, \varphi, \kappa)$, that parameterize the R_c^1 rotation matrix; the GPS positioning errors, $\vec{S}^1 = (s_x, s_y, s_z)^1$; and the $R_c^b(\Upsilon)$ IMU-to-camera relative orientation [boresight] calibration parameter¹. $R_b^{b'}$ is a constant rotation matrix.

2.3.1 Spatial Absolute Aerial Control: The functional models for the spatial absolute aerial control are

$$\vec{x}^1 + \vec{v}_x^1 = \vec{X}^1 + R_c^1(\Gamma) \cdot (\vec{A}^c + \vec{N}^c) + \vec{S}^1, \quad (1)$$

$$R_c^1(\Gamma) = R_{b'}^1 \cdot R_{b'}^{b'}(\chi + \vec{v}_\chi) \cdot R_b^{b'} \cdot R_c^b(\Upsilon) \quad (2)$$

for position and attitude respectively. Note, that in the above equation 2 for attitude control, in contrast to other formulations, the original INS/GPS-derived ψ, ϑ, γ IMU attitude angles can be directly used with no intermediate reparameterization steps.

2.3.2 Spatio-temporal Absolute Aerial Control: The functional models for the spatio-temporal absolute aerial control are:

$$\vec{x}^1 + \vec{v}_x^1 = \quad (3)$$

$$\vec{X}^1 + R_c^1(\Gamma) \cdot (\vec{A}^c + \vec{N}^c) + \vec{S}^1 - (\vec{v}^1 + \vec{v}_v^1) \cdot \Delta t,$$

$$R_c^1(\Gamma) = \quad (4)$$

$$R_{b'}^1 \cdot [R_{b'}^{b'}(\chi + \vec{v}_\chi) + \dot{R}_{b'}^{b'}(\chi + \vec{v}_\chi) \cdot \Delta t] \cdot R_b^{b'} \cdot R_c^b(\Upsilon).$$

In equation 3, the observables are the usual GPS or INS/GPS positions \vec{x}^1 and the INS/GPS linear velocities $\vec{v}^{1/2}$.

In equation 4, note the time derivative rotation matrix $\dot{R}_{b'}^{b'}$ that can be computed after the relationship

$$\dot{R}_{b'}^{b'}(\chi + \vec{v}_\chi) = R_{b'}^{b'}(\chi + \vec{v}_\chi) \cdot (\Omega_{ib'}^{b'} - \Omega_{il'}^{b'}),$$

where $\Omega_{ib'}^{b'}$ and $\Omega_{il'}^{b'}$ are observational auxiliary matrices. $\Omega_{ib'}^{b'} = \Omega_{ib'}^{b'}(\omega_x, \omega_y, \omega_z)$ is an angular velocity matrix where $(\omega_x, \omega_y, \omega_z)$ are the calibrated IMU angular velocities. $\Omega_{il'}^{b'} = \Omega_{il'}^{b'}(\lambda, \phi, \dot{\lambda}, \dot{\phi}, \omega_e)$ is an angular velocity matrix which depends on the known sensor position and on the Earth angular rate³. Δt is the multi-sensor time synchronization parameter which is used in both absolute control models (here) and in the spatio-temporal relative control models (section 2.4.2).

¹The boresight matrix can be parameterized in different ways. No parameterization is specified because it is not relevant to this research.

²Note that the symbol \mathbf{v} which denotes velocity is different from the symbol \mathbf{v} which denotes residuals.

³The $\Omega_{ib'}^{b'}$ matrix and the $\Omega_{il'}^{b'}$ matrix are well-known and can be found in any inertial navigation book as for example (Jekeli, 2001).

2.4 Relative Aerial Control Models

Relative aerial control functional models (spatial relative aerial control models (2.4.1) and spatio-temporal relative aerial control models (2.4.2)) involve the following observations and their residuals: the GPS- or INS/GPS-derived positions at epoch t_2 , $\vec{x}_2^1 = (x_2, y_2, z_2)^1$ and the Euler angles that parameterize the $R_{b'}^1$ rotation matrix at epoch t_2 , $\chi_2 = (\psi_2, \vartheta_2, \gamma_2)$. The involved parameters are: the camera projection centre at epoch t_1 , $\vec{X}_1^1 = (X_1, Y_1, Z_1)^1$; the Euler angles that parameterize the R_c^1 rotation matrix at epoch t_1 , $\Gamma_1 = (\omega_1, \varphi_1, \kappa_1)$; the camera projection centre at epoch t_2 , $\vec{X}_2^1 = (X_2, Y_2, Z_2)^1$; and the Euler angles that parameterize the R_c^1 rotation matrix at epoch t_2 , $\Gamma_2 = (\omega_2, \varphi_2, \kappa_2)$. The models of this section involve the following observational auxiliary values: the GPS- or INS-/GPS-derived positions at epoch t_1 , $\vec{x}_1^1 = (x_1, y_1, z_1)^1$ and the Euler angles that parameterize the $R_{b'}^1$ rotation matrix at epoch t_1 , $\chi_1 = (\psi_1, \vartheta_1, \gamma_1)$.

In the relative aerial control models, tPA (or tPVA in the case of spatio-temporal models) aerial control are introduced as observational auxiliary data (constant information) at epoch t_1 for numerical related issues.

2.4.1 Spatial Relative Aerial Control: The functional models for the spatial relative aerial control are:

$$\vec{x}_1^1 - (\vec{x}_2^1 + \vec{v}_{x_2}^1) = \quad (5)$$

$$\vec{X}_1^1 - \vec{X}_2^1 + [R_c^1(\Gamma_1) - R_c^1(\Gamma_2)] \cdot (\vec{A}^c + \vec{N}^c),$$

$$R_c^1(\Gamma_1) \cdot R_c^1(\Gamma_2) = \quad (6)$$

$$R_{b'}^1 \cdot R_{b'}^{b'}(\chi_1) \cdot R_{b'}^{b'}(\chi_2 + \vec{v}_{\chi_2}) \cdot R_{b'}^1.$$

Equations 5 and 6 are obtained from equations 1 and 2 respectively by straightforward algebraic operations. Note, that in equation 5 the positioning calibration parameter \vec{S}^1 has vanished and that in equation 6 the IMU-to-sensor boresight rotation matrix $R_c^b(\Upsilon)$ has vanished as well.

2.4.2 Spatio-temporal Relative Aerial Control: The functional models for the spatio-temporal relative aerial control are:

$$\vec{x}_1^1 - (\vec{x}_2^1 + \vec{v}_{x_2}^1) = \quad (7)$$

$$\vec{X}_1^1 - \vec{X}_2^1 + [R_c^1(\Gamma_1) - R_c^1(\Gamma_2)] \cdot (\vec{A}^c + \vec{N}^c) -$$

$$[\vec{v}_1^1 - (\vec{v}_2^1 + \vec{v}_{v_2}^1)] \cdot \Delta t$$

$$R_c^1(\Gamma_1) \cdot R_c^1(\Gamma_2) = \quad (8)$$

$$R_{b'}^1 \cdot [R_{b'}^{b'}(\chi_1) + \dot{R}_{b'}^{b'}(\chi_1) \cdot \Delta t] \cdot$$

$$[R_{b'}^{b'}(\chi_2 + \vec{v}_{\chi_2}) + \dot{R}_{b'}^{b'}(\chi_2 + \vec{v}_{\chi_2}) \cdot \Delta t]^T \cdot R_{b'}^1$$

In equation 7, the observables are the GPS or INS/GPS positions \vec{x}_2^1 and the INS/GPS linear velocities \vec{v}_2^1 at epoch t_2 . The INS/GPS linear velocities at epoch t_1 , \vec{v}_1^1 , are observational auxiliary values.

In equation 8, note the time derivative rotation matrices $\dot{R}_{b'}^{b'}$ that can be computed after the relationship

$$\dot{R}_{b'}^{b'}(\chi_1) = R_{b'}^{b'}(\chi_1) \cdot (\Omega_{ib'}^{b'} - \Omega_{il'}^{b'}),$$

$$\dot{R}_{b'}^1 (\chi_2 + \vec{v}_{\chi_2}) = R_{b'}^1 (\chi_2 + \vec{v}_{\chi_2}) \cdot (\Omega_{2_{ib'}}^{b'} - \Omega_{2_{il'}}^{b'}),$$

where $\Omega_{1_{ib'}}^{b'}$, $\Omega_{2_{ib'}}^{b'}$, $\Omega_{1_{il'}}^{b'}$, and $\Omega_{2_{il'}}^{b'}$ are auxiliary matrices. $\Omega_{1_{ib'}}^{b'} = \Omega_{ib'}^{b'}(\omega_{x_1}, \omega_{y_1}, \omega_{z_1})$ is an angular velocity matrix where $(\omega_{x_1}, \omega_{y_1}, \omega_{z_1})$ are the calibrated IMU angular velocities at epoch t_1 . $\Omega_{2_{ib'}}^{b'} = \Omega_{ib'}^{b'}(\omega_{x_2}, \omega_{y_2}, \omega_{z_2})$ is an angular velocity matrix where $(\omega_{x_2}, \omega_{y_2}, \omega_{z_2})$ are the calibrated IMU angular velocities at epoch t_2 . $\Omega_{1_{il'}}^{b'} = \Omega_{il'}^{b'}(\lambda_1, \phi_1, \lambda_1, \dot{\phi}_1, \omega_e)$ is an angular velocity matrix which depends on the known sensor position and on the Earth angular rate at epoch t_1 . $\Omega_{2_{il'}}^{b'} = \Omega_{il'}^{b'}(\lambda_2, \phi_2, \lambda_2, \dot{\phi}_2, \omega_e)$ is an angular velocity matrix which depends on the known sensor position and on the Earth angular rate at epoch t_2 .

3 CONCEPT VALIDATION RESULTS

In order to analyse the overall feasibility and, somewhat, validate the concepts introduced in the previous sections, some of the newly formulated models were implemented and tested with actual data against the classical spatial absolute control models whose results played the reference role. More precisely, the functional model of equation 3 was tested against the model of equation 1 (section 3.1, “Spatial Absolute vs Spatio-temporal Absolute”) and the functional models of equations 5, 6 were tested against the reference models of equations 1, 2 respectively (section 3.2, “Spatial Absolute vs Spatial Relative”). For this purpose the “Pavia block” (provided to the Institute of Geomatics by Prof. Vittorio Casella, Facoltà di Ingegneria, Università di Pavia, Italy) was used. The configuration characteristics of the block are summarized in table 2 and its layout can be seen in figure 1. The Pavia block provided all necessary data for the validation purposes mentioned with the exception of the INS/GPS-derived linear velocities and calibrated angular velocities that were not available to the author at the moment of setting up the experiments. To overcome this, the correct INS/GPS-derived velocities were approximated by numerically differentiating the INS/GPS-derived positions at the image exposure time epochs with the three-point stencil method.

Scale	1:8000
Flying height	1200 m
No. of strips	11 (7+4)
No. of images per strip	≈ 10
No. of photo-observations per image	≈ 30
No. of Ground Control Points (GCP)	8
No. of Ground Check Points (CP)	24
No. of images	131
No. of photo-observations	4167
No. of tie-points	477
Overlap	≈ 60% × 60%

Table 2: Pavia block configuration characteristics.

3.1 Spatial Absolute vs Spatio-temporal Absolute

The goal of this section is to validate whether the multi-sensor time synchronization parameter Δt can be significantly estimated with a sufficient precision and to provide

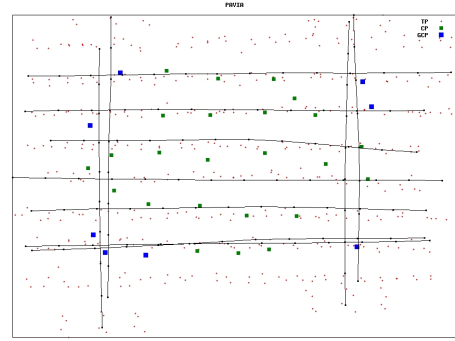


Figure 1: Pavia block layout.

Test	Model	Shift	Velocity
A	Spatial	1 per strip (11)	-
B	Spatial	1 per block	-
C	Spatio-temporal	1 per strip (11)	ct-actual
D	Spatio-temporal	1 per block	ct-actual
E	Spatio-temporal	1 per strip (11)	non-ct

Table 3: Absolute spatial and spatio-temporal block configurations.

some insight on the corresponding required block configurations and, eventually, mission configurations. The validation consists on the controlled determination of a significant and precise Δt that preserves or improves the quality of the block which is measured by the point determination accuracy at the ground check points (CPs).

As it is to be expected (equation 3), for approximately constant velocities, the GPS positioning error calibration parameters \vec{S}^1 —the popular GPS “shift” parameters— and the time synchronization parameter Δt are highly correlated if the classical block configurations of one “shift” per strip are used. This is due to the constant-computed velocities. Therefore, to a large extent, the concept validation problem reduces to the analysis of the conditions under which, the Δt and the various \vec{S}^1 can be de-correlated. For this purpose, the data were perturbed with time synchronization errors and five block/mission configurations were analyzed as described in table 3. In the table, ct-actual refers to the more or less constant actual velocities and non-ct refers to the perturbed linear velocities where the strips’ ends are flown at a different speed while taking the first and last images. For all these configurations or tests, the observables’ precisions at the $1-\sigma$ level are listed in table 4 where IC denotes photogrammetric image coordinates observations, P position, A attitude and V velocity. Note that for the PA control the sequence of observations is $(X, Y, Z, \psi, \vartheta, \gamma)$.

The tests results are shown in table 5. The first column

Observable	σ	Units
IC	(5, 5)	um
GCP	(5, 5, 7)	cm
INS/GPS PA	(5, 5, 7, 8, 5, 5)	cm, mdeg
INS/GPS V	(5, 5, 5)	mm/s

Table 4: Observables’ precisions.

contains the test identifier, the second one the Root-Mean-Square (RMS) of the ground coordinate differences with respect the check points (CP); the third one the estimated standard deviations of the images' exterior orientation (EO) parameters; the fourth one the estimated standard deviations of the object points (TP); and the last one the estimated standard deviation of the time synchronization parameter.

Test	CP (mm) RMS	EO (mm) σ	TP (mm) σ	ΔT (ms) σ
A	(36, 27, 25)	(35, 36, 32)	(29, 30, 47)	—
B	(35, 25, 28)	(35, 35, 32)	(29, 30, 47)	—
C	(36, 27, 25)	(35, 36, 32)	(29, 30, 46)	2.2
D	(34, 24, 27)	(35, 35, 32)	(29, 30, 47)	0.1
E	(35, 26, 25)	(35, 36, 32)	(28, 30, 46)	0.2

Table 5: Absolute spatial and spatio-temporal test results.

The analysis of table 5 reveals that the systematic GPS aerial control errors can be absorbed with just one shift parameter (compare rows A and B) which corresponds, for instance, to situations where the GPS reference receiver is close to the block area. This has allowed to significantly estimate (test D, functional model of equation 3) the Δt parameter with just one shift parameter for the entire block with a precision of 0.1 ms which translates to less than 1 cm in the object space. Moreover, the estimated Δt maintains the block quality level as proven by the correct results at the check points. If one shift parameter per strip is introduced, then the time synchronization parameter cannot be estimated at the required precision level —2.2 ms or 18 cm in the object space— and, although the CP, EO and TP columns show correct values, the configuration is labelled as “non acceptable.” However, experience tells that enforcing the use of just one single shift parameter per block does not make sense in many —if not most— of cases. In order to circumvent this problem, the block data were “manipulated” to simulate the case of strips flown at different velocities at their ends while taking the first and last images (test E). In this case, the Δt parameter and 11 shift parameters, one per strip, could be significantly and precisely estimated ($\sigma_{\Delta T} = 0.2$ ms).

The presented preliminary results are encouraging and indicate that if, as a result of windy weather or of simple aircraft velocity “maneuvers,” the constant velocity limitation is broken, multi-sensor time calibration as presented in this paper is feasible. Last, note that the used velocities were not obtained from INS/GPS data and that the observation equation 4 was not used. In other words, there is room for further improvement.

3.2 Spatial Absolute vs Spatial Relative

The main goal of this section is to validate the aerial relative control models of equations 5 and 6. The validation consists on the comparative analysis of a standard ISO block configuration with absolute spatial aerial control and a new one with relative control via the RMS of coordinate differences at check points. For this purpose, the Pavia block was used again. The observations' precisions are described in table 6 which is largely self-explanatory.

Observable	σ	Units
IC	(5, 5)	um
GCP	(8, 8, 10)	cm
INS/GPS Abs PA	(7, 7, 11, 8, 5, 5)	cm, mdeg
INS/GPS Rel PA	(4, 4, 8, 2.7, 2.7, 2.7)	cm, mdeg

Table 6: Observables' precisions.

Test	CP (mm) RMS	EO (mm,mdeg) σ	TP (mm) σ
Abs	(35, 27, 26)	(39, 40, 35, 1.3, 1.3, 0.8)	(32, 33, 49)
Rel	(33, 26, 27)	(39, 42, 46, 1.4, 1.2, 0.8)	(35, 36, 58)

Table 7: Absolute vs relative aerial control test results.

One of the advantages of the INS/GPS relative control is its high short term precision. Accordingly, the INS/GPS relative control precisions have been [conservatively] set to values consistent with the photogrammetric base and the IMU used in the Pavia block (row 'INS/GPS Rel PA' of table 6).

The results are shown in table 7. The first column contains the test configuration (Abs and Rel refer to the spatial aerial absolute and relative control models respectively); the rest of the columns are similar to those in table 5. On the one hand, the results confirm that ISO can be performed without shift and boresight calibration parameters at the price of larger estimated standard deviations in the height components of ground points (20% worse) and projection centers (30% worse). This is thought to be due to the less favorable error propagation —a somewhat weaker geometry or block *Bierbauch* effect— of relative control. The predicted errors notwithstanding, the results at the ground check points are even [insignificantly] better with relative aerial control. In the author's opinion, these are remarkable results. Indeed, for everyday practical use, the relative control formulation is simpler and less error prone than the absolute one.

Another potential expected advantage of the relative aerial control models is the mitigation of undetected GPS cycle slips effects. For this purpose, the INS/GPS-derived positions of half a central strip were largely perturbed with 50 cm shifts. Figures 2 and 3 show the coordinate differences at check points with the absolute and relative aerial control models respectively. As it can be seen, the relative aerial control models are less sensitive than the absolute aerial control models.

Moreover, the performance of the absolute aerial control models and the relative aerial control models after removed the gross-errors (detected with automated data-snooping) is shown in the table 8. The columns of this table are the same as the columns of the table 7. Again, the RMS of the coordinate differences at check points indicate that the relative control models behave better than the absolute ones.

Test	CP (mm) RMS	EO (mm,mdeg) σ	TP (mm) σ
Abs	(41, 42, 29)	(40, 41, 36, 1.3, 1.3, 0.8)	(33, 34, 50)
Rel	(33, 26, 27)	(39, 42, 46, 1.4, 1.3, 0.8)	(35, 36, 58)

Table 8: Absolute vs Relative aerial control test results.

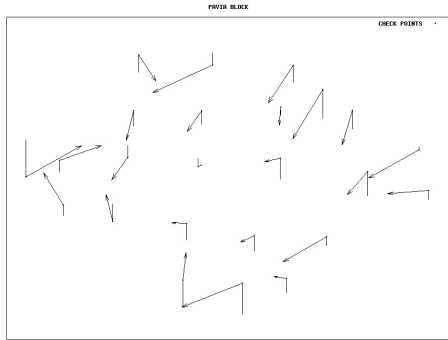


Figure 2: Absolute-estimated coordinate differences at check points of perturbed data test.

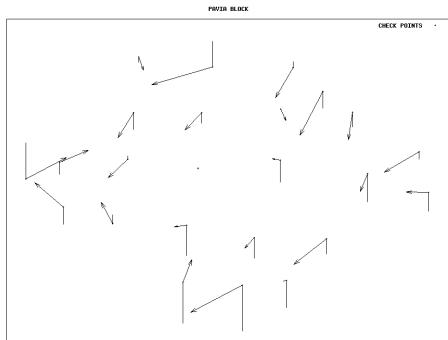


Figure 3: Relative-estimated coordinate differences at check points of perturbed data test.

These preliminary results suggest that the relative control models are more robust and reliable than the absolute aerial control model in front of undetected GPS cycle slips even if the gross-errors are removed from the data.

4 CONCLUSIONS AND FURTHER RESEARCH

This paper has introduced new mathematical functional models (equations 2, 3, 4, 5, 6, 7 and 8) for the spatial and spatio-temporal modeling of the GPS- and INS/GPS-derived aerial control data. Using actual data and perturbed actual data, the essential subset of the new functional models (equations 3, 4, 5 and 6) have undergone a successful preliminary, proof-of-the-concept testing.

In the case of spatial relative aerial control models (equations 5 and 6), the expected advantages have been demonstrated with the first results using actual data. The spatial relative aerial control models eliminates the IMU-to-sensor relative orientation matrix and the GPS positioning error parameters without loss of accuracy and with a moderate loss of precision. Moreover, this model seems to mitigate the effects of undetected GPS cycle slips “better” — in the sense of reliability and robustness — than the spatial absolute aerial control models.

In the case of spatio-temporal absolute aerial control models (equations 3 and 4), the expected advantages are being tested with actual and perturbed data. The first results in-

dicate that the time synchronization parameter can be estimated at the tenth of a millisecond precision level. New block configurations have been identified in order to estimate the multi-sensor time synchronization and the GPS positioning error parameters simultaneously.

The spatio-temporal relative aerial control models are not yet implemented. But, the results of the spatio-temporal absolute aerial control models and spatial relative aerial control models indicate that this approach could be even more reliable and robust, if a few consecutive images could be taken at different velocities. This implementation is planned together with the use of actual data to demonstrate the potential of the temporal calibration models.

REFERENCES

- Ackermann, F. and Schade, H., 1993. Application of GPS for aerial triangulation. *Photogrammetric Engineering and Remote Sensing* 59(11), pp. 1625–1632.
- Blázquez, M. and Colomina, I., 2008. On the Use of Inertial/GPS Velocity Control in Sensor Calibration and Orientation. In: *Proceedings of the EuroCOW 2008, Castelldefels, ES*.
- Colomina, I., 1999. GPS, INS and Aerial Triangulation: what is the best way for the operational determination of photogrammetric image orientation? In: *International Archives of Photogrammetry and Remote Sensing, ISPRS Conference “Automatic Extraction of GIS Objects from Digital Imagery”, Vol. 32*, pp. 121–130.
- Frieß, P., 1991. Aerotriangulation with gps-methods, experience, expectation. In: *Proceedings of the 43rd Photogrammetric Week, Stuttgart, DE*.
- Jekeli, C., 2001. *Inertial navigation systems with geodetic applications*. Walter de Gruyter, Berlin, New York.
- Lucas, J., 1987. Aerotriangulation without ground control. *Photogrammetric Engineering and Remote Sensing* 53(3), pp. 311–314.
- Schwarz, K., Chapman, M., Cannon, M. and Gong, P., 1993. An integrated INS/GPS approach to the georeferencing of remotely sensed data. *Photogrammetric Engineering and Remote Sensing* 59(11), pp. 1667–1674.

5 ACKNOWLEDGEMENTS

The models are implemented and tested with the generic network adjustment platform GENA from GeoNumerics (Barcelona, Spain). The block data were made available by Prof. Vittorio Casella (Università di Pavia). Last, but not least, the discussions held with Dr. Ismael Colomina (Institute of Geomatics) are kindly acknowledged.